HETEROCYCLES, Vol. 104, No. 9, 2022, pp. -. © 2022 The Japan Institute of Heterocyclic Chemistry
Received, 13th June, 2022, Accepted, 25th July, 2022, Published online, 29th July, 2022
DOI: 10.3987/COM-22-14696

THE CONTINUOUS-FLOW SYNTHESIS OF 1*H*-INDAZOLES VIA REACTION OF *o*-FLUOROBENZALDEHYDES WITH *tert*-BUTYL CARBAZATE UNDER HIGH TEPERATURE

Wenjie Ye,[a] Kai Zhu,[b] Yiping Huang,[b] Chuansong Duanmu,[a] Yanxing Li,[a] Jin Li,[a] Weichuan Xu,[a] and Feng Zhou[a]*

[a] National & Local Joint Engineering Research Center for Deep Utilization Technology of Rock-salt Resource, Faculty of Chemical Engineering, Huaiyin Institute of Technology, Huai'an 223003, P. R. China. [b] China Construction Industrial & Energy Engineering Group Co., Ltd., 6 Wenlan Road, Qixia District, Nanjing 210023, P. R. China. E-mail: zhoufeng@hyit.edu.cn.

Abstract – Large amounts of 1*H*-indazoles have been developed and widely used in the production of diverse drugs. The reaction of 4-bromo-2,6-difluorobenzaldehyde with *tert*-butyl carbazate was selected as model transformation for the application of continuous-flow strategy to realize the efficient syntheses of 1*H*-indazoles in a highly controlled and safe manner. Various conditions (reaction temperature, residence time, solvent amount, the amount of *tert*-butyl carbazate, water content) were investigated under continuous-flow conditions to elucidate the benefits of using the continuous-flow strategy. The Box-Behnken design in response surface methodology was employed for the optimization of reaction conditions, and over 85% yield of 6-bromo-4-fluoro-1*H*-indazole could be achieved. Furthermore, the generality of the reaction conditions found optimal for the synthesis of 6-bromo-4-fluoro-1*H*-indazole was evaluated for the synthesis of several different 1*H*-indazoles.

INTRODUCTION

The organic compounds possessing indazole heterocyclic core tend to be equipped with diverse levels of biological and pharmaceutical activities. Large amounts of 1*H*-indazole derivatives have been developed and widely used in anti-cancer,[1] anti-inflammatory,[2] anti-tumor,[3] anti-HIV[4] and other drugs. Besides, 1*H*-indazole derivatives also can be used for the production of various dyes.[5] The many practical

applications of 1*H*-indazoles in industry have inspired much interest of researchers in their syntheses for a long time.

Researchers have tried to achieve the efficient production of 1*H*-indazoles in many ways, but they have generally focused on modifying the synthetic routes. One of the classical methods used to synthesize 1*H*-indazoles is through the condensation of *o*-fluorobenzaldehydes with hydrazines.[6] The 1*H*-indazoles also can be synthesized via diazotization or nitrosation of *o*-alkyl-substituted anilines.[7,8] The 1,3-dipolar cycloadditions of diazomethanes with benzynes is another important route for the preparation of 1*H*-indazoles.[9] In recent years, transition-metal catalysis has been developed into one of the most important methods to synthesize 1*H*-indazoles. Many attempts focusing on the development of more effective transition-metal catalysts have been conducted to optimize this method. For example, Glorius et al. developed a novel synthesis route of 1*H*-indazoles via Rh(III)-catalyzed C-H activation/C-N bond formation and Cu-catalyzed N-N bond formation in which aryl imidates and organo azides served as starting materials.[10] Among the above synthetic routes, the condensation of *ortho*-substituted aryl aldehydes with hydrazines is regarded as a particularly straightforward and attractive manner to synthesize the 1*H*-indazoles from the economic perspective.

The classical synthetic route of 1*H*-indazoles via condensation of *o*-fluorobenzaldehydes with excess hydrazine hydrate usually should be operated under high temperature with the intermittent mode of batch reactor.[11-17] Hydrazine hydrate (with a relatively low boiling point of 120 ^{o}C) should be treated with extreme caution due to its high toxicity, potential carcinogenicity, and severe corrosivity. The volatile reaction component in hydrazine hydrate is extremely readily to accumulate in the headspace of a batch reactor under high temperature, which can result in violent explosions. Thus, this synthetic route could not be considered practical for large-scale preparation of 1*H*-indazoles over process safety concerns. Flow chemistry technology has been considered by us to develop a safe and reliable process for improving the high-risk synthetic route of 1*H*-indazoles based on the condensation of *o*-fluorobenzaldehydes with hydrazines, due to its significant advantages in terms of heat and mass transfer, manipulation of reaction condition, process efficiency, productivity and safety.[18-20] For example, the continuous-flow microreactor has been used in the pharmaceutical industry to handle the chemical reagents with high security risk, e.g., diazomethane, in a safe and controlled manner.[21] Significantly reduced reaction time can be achieved in the continuous-flow microreactor, in which the reaction system can be kept in a superheated status safely and an extended operation temperature range can be adopted. The continuous-flow microreactor applied for the reaction operated under harsh conditions usually constructed by the robust metal alloys, however, the hydrazine hydrate may face the problem of partial decomposition in the presence of metals.[22] The

tert-butyl carbazate is an effective alternative reagent of hydrazine hydrate, which can avoid the limitations of reactor material and further eliminate the safety risk brought by the use of hydrazine hydrate.

In this work, the reaction of 4-bromo-2,6-difluorobenzaldehyde (SM) with *tert*-butyl carbazate to prepare 6-bromo-4-fluoro-1*H*-indazole (BFI) was chosen as the model transformation for a thorough study of the synthesis process of 1*H*-indazoles based on the classical route. Application of continuous-flow strategy under high temperature was exploited to obtain an improved and more efficient process for producing 1*H*-indazoles. Various reaction conditions (reaction temperature, residence time, solvent amount (*V-ratio*), the amount of *tert*-butyl carbazate (*M-ratio*), water content (W_C)) were investigated under continuous-flow mode to elucidate the benefits of using the continuous-flow strategy. The Box-Behnken design in response surface methodology was employed to obtain the optimized reaction conditions. Besides, the generality of the reaction conditions found optimal for the synthesis of 6-bromo-4-fluoro-1*H*-indazole was evaluated for the reaction of several different substituted *o*-fluorobenzaldehydes with *tert*-butyl carbazate.

RESULTS AND DISCUSSION

SOLVENT SCREENING IN A SEALED AUTOCLAVE

The synthesis of 6-bromo-4-fluoro-1*H*-indazole (BFI) via reaction of 4-bromo-2,6-difluorobenzaldehyde (SM) with *tert*-butyl carbazate consists primarily of the following three steps (Scheme 1): SM first reacts with the *tert*-butyl carbazate to generate the aromatic Boc-protected hydrazone (ABPH), and then the thermal deprotection of Boc groups in ABPH can be realized to form the aryl hydrazone (AZ), and finally the aryl hydrazone is cyclized to yield the anticipated BFI product. The formation of ABPH can be carried out around room temperature and an obvious equilibrium between the SM with ABPH was found in our batch experiment at 20 ^{o}C. However, the thermal deprotection of Boc groups and the cyclization of AZ are considered to be performed under high temperature, in which the continuous-flow strategy can show significant advantage. [23]

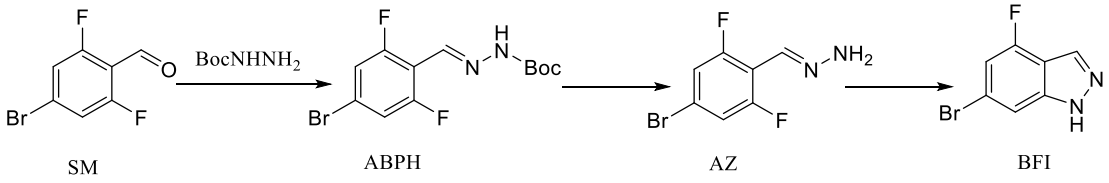

Scheme 1. The synthesis of BFI via reaction of SM with *tert*-butyl carbazate

Table 1. Solvent screening[a]

Entry	solvent	solubility	B.P. [°C]	BFI [%][b]
1	NMP	√	202	90.9
2	DMSO	√	189	30.7
3	EtOH	X	78	30.6
4	DMF	√	153	75.3
5	*i*-PrOH	X	82	33.7
6	THF	√	66	76.1
7	glycol	X	197	87.8
8	MeOH	X	65	50.8
9	MeCN	X	82	67.5
10	acetone	√	57	15.1

[a] Conditions: *V-ratio* 20, *M-ratio* 1.1, 30 min at 200 °C, 0.8 mL reaction mixture in 2 mL sealed autoclave.

[b] Determined by HPLC peak area integration at 220 nm.

In order to identify appropriate solvent amenable to flow process, a solvent screen was initially performed in a sealed autoclave. To determine solvent consumption, the ratio between the volume of the solvent to the mass of SM was used, which was defined as a *V-ratio*. *M-ratio*, defined as the molar ratio of *tert*-butyl carbazate to SM, was used to determine the amount of *tert*-butyl carbazate being used. Typically, an initial reaction solution with *V-ratio* of 20 and *M-ratio* of 1.1 was heated to 200 °C for 30 min in a sealed autoclave. The autoclave was fixed in a turntable and rotated at 30 rpm to ensure effective mixing and heat/mass transfer. This screening reveals that NMP shows the good stability, solubility and reactivity toward the synthesis of BFI (Entry 1, Table 1). Alcohol solvents (Entries 3,5,7 and 8, Table 1) including MeOH, EtOH, *i*-PrOH and glycol cannot dissolve the SM well, although up to 87.8% BFI area percent in the reaction mixture could be achieved when the glycol was selected as solvent. The solvent of acetonitrile (Entry 9, Table 1) not only could not dissolve the SM well, but also showed the significant formation of impurities. The solvents of DMSO and acetone (Entries 2 and 10, Table 1) showed low product area percent and massive formation of impurities, which confirmed the poor stability of the solvents under high temperature.[24,25] DMF and THF (Entries 4 and 6, Table 1) both behaved relatively steadily in the synthesis of BFI, but compared with the solvent of NMP the relatively low BFI area

percent diminished its suitability for our purposes. Therefore, we considered NMP as the solvent of choice for the prospective flow process.

CONTINUOUS-FLOW MODE FOR THE SYNTHESIS OF 1*H*-INDAZOLES

While the reaction performance investigated in the sealed autoclave has certain reference value, large difference between the batch and continuous-flow mode still presents owning to the free volume in the autoclave and the vaporization characteristics of reaction components under high temperature. Next, we turned our attention to the translation of batch reaction towards a continuous-flow synthesis of BFI.

INFLUENCE OF THE REACTION TEMPERATURE AND RESIDENCE TIME

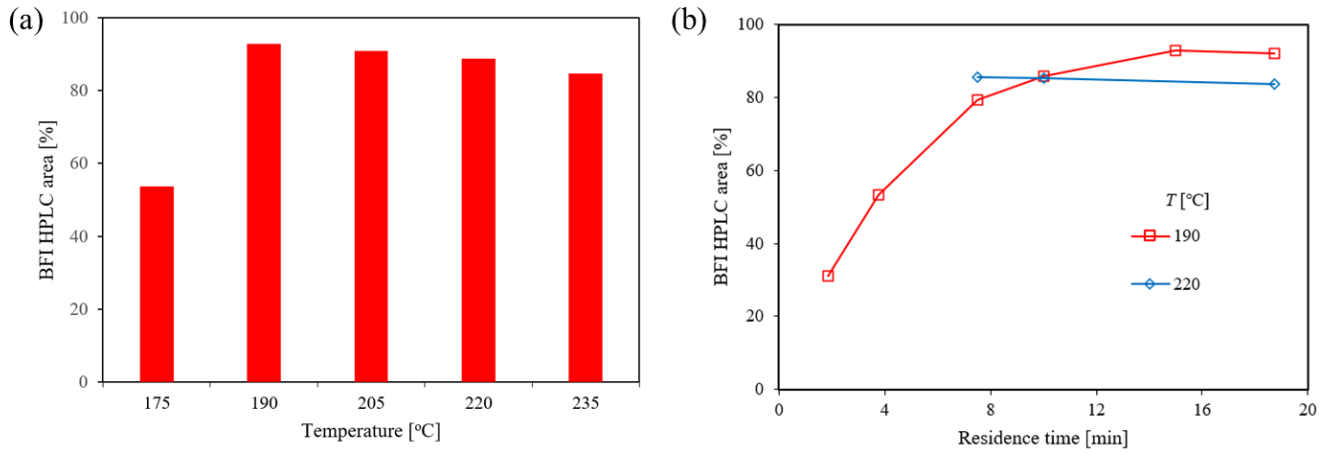

Figure 1. Investigation of the residence time and reaction temperature dependence for the synthesis of BFI under continuous-flow conditions.

Reaction conditions: (a) *V-ratio* 20, *M-ratio* 2, 15 min at 175~235 °C. (b) *V-ratio* 20, *M-ratio* 2, 3.8~18.8 min at 190~220 °C.

Considering that both the deprotection of Boc groups in ABPH and cyclization of AZ (Scheme 1) should be operated under high temperature, temperatures in the range of 175~235 °C were screened at 750 psi to elucidate the temperature dependence of the synthesis of BFI under continuous-flow mode (Figure 1(a)). Safer and more reliable process can be guaranteed by the continuous-flow mode under high temperature compared with its batch counterparts. Elevation of the temperature could accelerate the reaction but did not cause a continuous increase in the formation of BFI. As the temperature was increased from 175 to 235 °C, the BFI area percent increased from 53.7% to 92.8% and then decreased to 84.7%. Under high temperature the hydroxylation of the reaction components to form phenolic compounds may take place due to the formation of water in the thermal deprotection of Boc-group. Besides, the cross condensation of AZ with SM or BFI also may take place under high temperature, resulting in the decrease of BFI area percent. The obvious decrease of BFI area percent at high temperature (>190 °C) indicated that an appropriate temperature was required to accelerate the reaction rate while improving the selectivity for

the synthesis of BFI. Figure 2(b) demonstrates the influence of residence time on the formation of BFI. With increasing residence time at 190 °C, the BFI area percent increases quickly and then slightly decreases, while the BFI area percent decreases from 85.6% to 83.5% with increasing residence time from 7.5 min to 18.8 min at 220 °C, indicating that a shorter residence time is beneficial for achieving better formation of BFI at higher reaction temperature.

INFLUENCE OF THE AMOUNT OF tert-BUTYL CARBAZATE (M-RATIO)

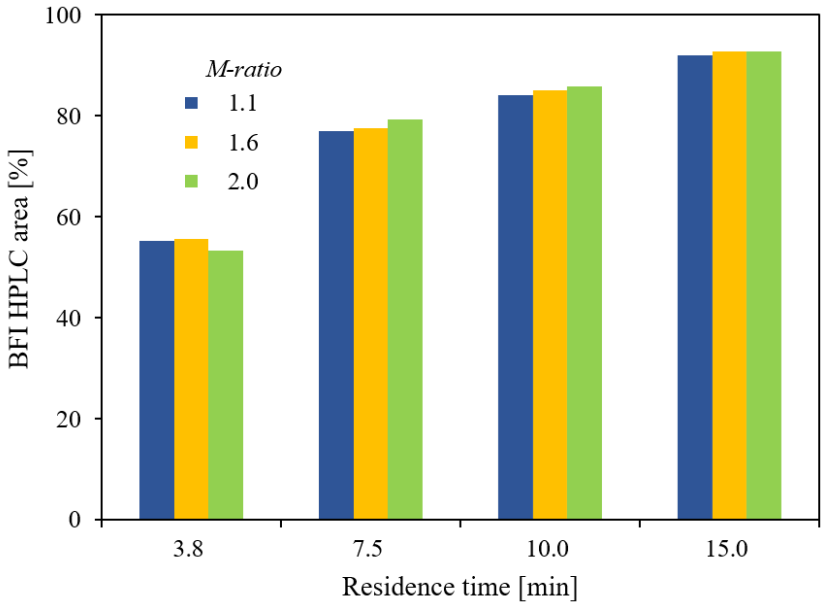

Figure 2. Screening of the *M-ratio* for the synthesis of BFI under continuous-flow conditions. Reaction conditions: *V-ratio* 20, *M-ratio* 1.1~2.0, 3.8~15.0 min at 190 °C.

The screening of the *M-ratio* in the range 1.1~2.0 at various residence times showed that the formation of BFI was not sensitive to an increase in the *M-ratio*; only slight differences in the BFI area percent were observed when the *M-ratio* was increased from 1.1 to 2.0 (Figure 2). This is easy to understand that although the increase of the *M-ratio* can promote the conversion of SM to ABPH, the formation rate of BFI is significantly restricted by the reaction rate of thermal deprotection of Boc groups and the cyclization of AZ. Besides, a further increase of *M-ratio* to 3.0 resulted in the severe blockage of reactor channel. Thus, a slight excess of *tert*-butyl carbazate (e.g., an *M-ratio* of 1.1) was adequate for the preparation of BFI.

INFLUENCE OF THE WATER CONTENT (W_C)

Hydrazine in the conventional experiments were usually used as aqueous solutions. The water is also a product during the generation of hydrazone in our reaction process. Therefore, it was necessary to investigate the effect of the water content (W_C) on the reaction.

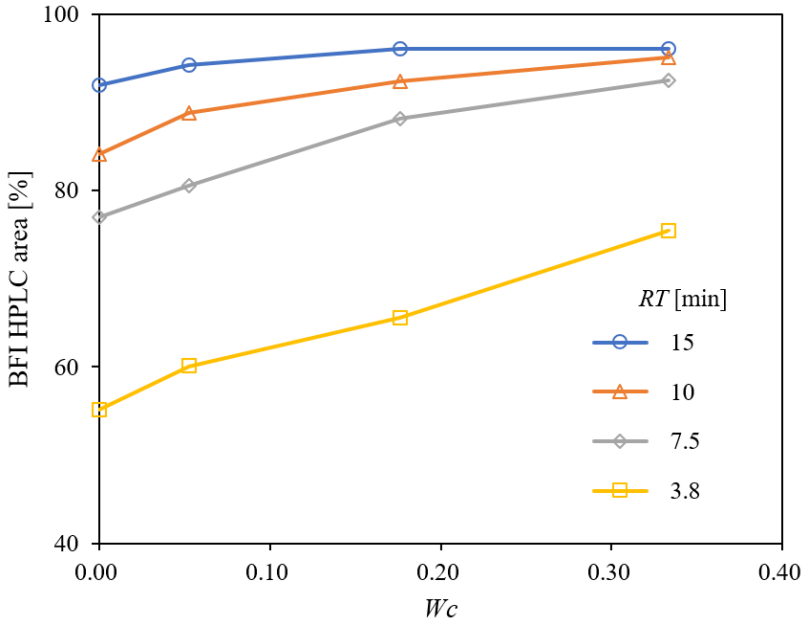

Figure 3. Effect of the W_C on the synthesis of BFI under continuous-flow conditions. Reaction conditions: *V-ratio* 20, *M-ratio* 1.1, 3.8~15 min at 190 °C.

The water content W_C is defined as the volume ratio of water to NMP in the solvent. In our experiments, elevating W_C from 0 to 0.33 could effectively promote the formation of BFI (Figure 3). It might be the reason that hydronium ions formed by the dissociation of water under high temperature could serve as a catalyst in the present system, which could promote the deprotection of ABPH.[26] However, the increase of W_C obviously aggravated the blockage in the reactor channel. For example, as the residence time was increased from 3.8 min to 15 min with a W_C of 0.33, the obvious blockage phenomenon could be observed, and it was necessary to switch the three-way ball valve to introduce the solvent NMP to clean the reactor channel for each change of residence time. This phenomenon may have been the case because the reaction system is a complex competitive reaction system and the increase of W_C will reduce the solubility of some intermediates or byproducts. Therefore, although the increase of W_C can promote the reaction, but it is not considered as a preferred choice to improve the synthesis of BFI due to the existence of blockage risk.

FINE-TUNING OF THE CONDITIONS USING RESPONSE SURFACE METHOD

A well-known statistical method for formulating and optimizing processes is response surface methodology (RSM).[27,28] According to the above investigation on the process parameters, a standard RSM with three level three-factor Box-Behnken design was applied in this work and the range and levels listed in Table 2 were applied to generate the experimental design matrix (Table 3) using Design Expert software. A total of 17 experimental runs were suggested by the design. Runs 3, 4, 6, 9 and 16 at the center point of the design were used to determine the experimental error. Experiments were carried out

following the design, and the responses were listed in Table 3. The experimental results were analyzed by the response surface methodology according to the a second-order polynomial equation. Analysis of variance (ANOVA) for the response surface quadratic model was applied to investigate the fitness and significance of the model, the precision of the model, the effects of the individual variables, and interactive effects on the response. The result (ANOVA) is shown in Table 4.

Table 2. Levels and Range of independent variables for experimental design

Level	Coded level	Uncoded level		
		A: *T* [°C]	B: *RT* [min]	C: *V-ratio*
Low	-1	175	5	8
Mid	0	190	10	14
High	1	205	15	20

Table 3. Experimental design matrix and results[a]

Run	Actual level of variables			HPLC area [%]	
	T [°C]	*RT* [min]	*V-ratio*	BFI Observed	BFI Predicted
1	190	15	8	91	89.9
2	205	15	14	94.6	95.2
3[b]	190	10	14	86.8	86.9
4[b]	190	10	14	87.7	86.9
5	205	10	8	95.1	95.7
6[b]	190	10	14	85.9	86.9
7	190	15	20	92.0	92.0
8	190	5	20	69.5	70.7
9[b]	190	10	14	87.9	86.9
10	190	5	8	77.8	77.9
11	175	10	8	62.4	62.9
12	205	5	14	92.1	91.5
13	175	5	14	47.0	46.5
14	175	15	14	75.4	76.1

15	175	10	20	61.7	61.1
16[b]	190	10	14	86.2	86.9
17	205	10	20	92.9	92.4

[a] A Box-behnken design with five replicates of the center point. [b] Center points.

Table 4. ANOVA for response surface quadratic model

Source	Sum of Squares	df	Mean Square	F-value	p-value	
Model	3081.86	9	342.43	283.33	< 0.0001	significant
A-*T*	2054.41	1	2054.41	1699.86	< 0.0001	
B-*RT*	554.45	1	554.45	458.76	< 0.0001	
C-*V-ratio*	13.01	1	13.01	10.76	0.0135	
AB	167.70	1	167.70	138.76	< 0.0001	
AC	0.5625	1	0.5625	0.4654	0.5170	
BC	21.62	1	21.62	17.89	0.0039	
A^2	211.51	1	211.51	175.00	< 0.0001	
B^2	27.11	1	27.11	22.43	0.0021	
C^2	13.45	1	13.45	11.13	0.0125	
Residual	8.46	7	1.21			
Lack of Fit	5.32	3	1.77	2.26	0.2237	not significant
Pure Error	3.14	4	0.7850			
Cor Total	3090.32	16				

A Model F-value of 283.33 indicates that the model is significant. There is only a 0.01% chance that an F-value this large could occur due to noise. An p-value of less than 0.0500 indicates that terms in the model are significant. The model terms A, B, C, AB, BC, A^2, B^2, C^2 are significant in this case. A value greater than 0.1000 indicates that the model terms are not significant. Due to the highest F-value, it is observed that among the three individual variables studied, reaction temperature (A) had the largest effect on the BFI area percent, followed in order by the residence time (B), and *V-ratio* (C). The Lack of Fit F-value of 2.26 implies the Lack of Fit is not significant relative to the pure error. There is a 22.37% chance that a Lack of Fit F-value this large could occur due to noise. The determination coefficient (R^2) value is 0.9973. In other words, only 0.27% of the total variability is not explained by the regressions in the model and may be caused by human error or experimental errors. The Predicted R^2 of 0.9709 is in

reasonable agreement with the Adjusted R^2 of 0.9937. Adequate precision measures the ratio of the signal-to-noise, and when the ratio is greater than 4, the model is a desirable one. Our ratio of 58.411 thus shows an adequate signal; hence, this model can be used to navigate the design space.

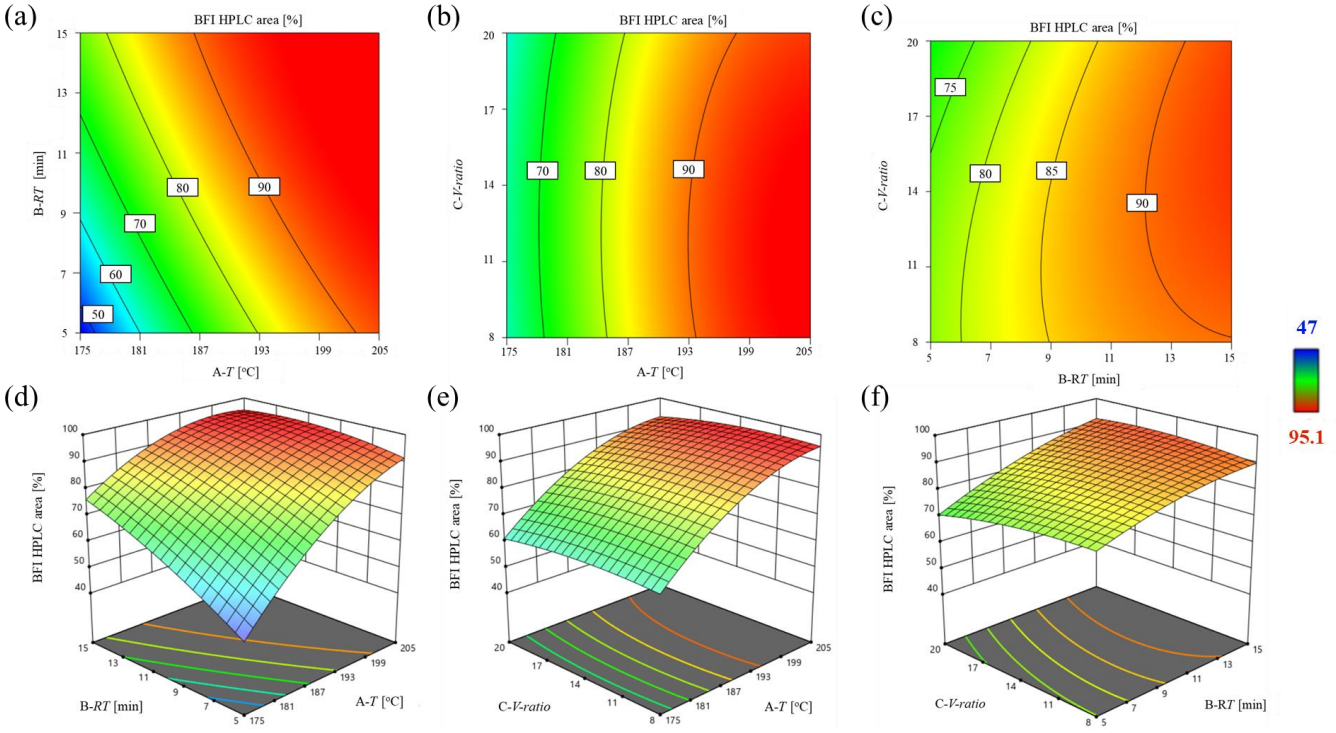

Figure 4. Contour (a/b/c) and three-dimensional response surface (d/e/f) plot of the influence of the reaction temperature, residence time and *V-ratio* on the area percent of BFI

A clearer interpretation of the effects of variable interaction on the area percent of BFI in the reaction mixture can be seen by examining the response 3D plots and contour plots (Figure 4). 3D surface plots show the extent of variation of the responses with single and combined effects of two factors (keeping other factor at zero level) while 2D contour representation of the 3D surface helps to identify the major interactions that take place between the process variables from the circular or elliptical nature of the contours. Our foremost objective of this study is to obtain the optimized reaction conditions to maximize the formation of BFI. Based on the constraints we set; software generated optimized reaction conditions for the optimized response. The most desirable reaction condition for maximum area percent of BFI has been found as following reaction temperature 205 ^{o}C, residence time 11.1 min, and *V-ratio* 12.1.

LONG-TIME OPERATION STABILITY TEST

As discussed above, the optimized reaction condition for maximum area percent of BFI has been obtained using response surface methodology. A long-time operation stability test (>12 h) under the optimized reaction condition was carried out to verify the process reliability (Figure 5). 15 Fractions of reaction

mixtures at different time intervals were collected and analyzed by HPLC. Of these fractions, an average BFI area percent of 96.4% could be obtained in the HPLC analysis. The reaction system could be operated stably without obvious blockage. Besides, the reaction mixtures from two different periods (1 h) were collected and quantitatively analyzed using the external standard method. Over 85% yield of BFI could be achieved under optimized condition (Table 5). Compared with the conventional batch process reported in the literature,[12] in which the title compound BFI can achieve 90% yield through a one-pot two-step sequence with an operation time of over 30 h, our work can provide the advantages of easier operation and shorter operation time while obtain a yield of > 85%.

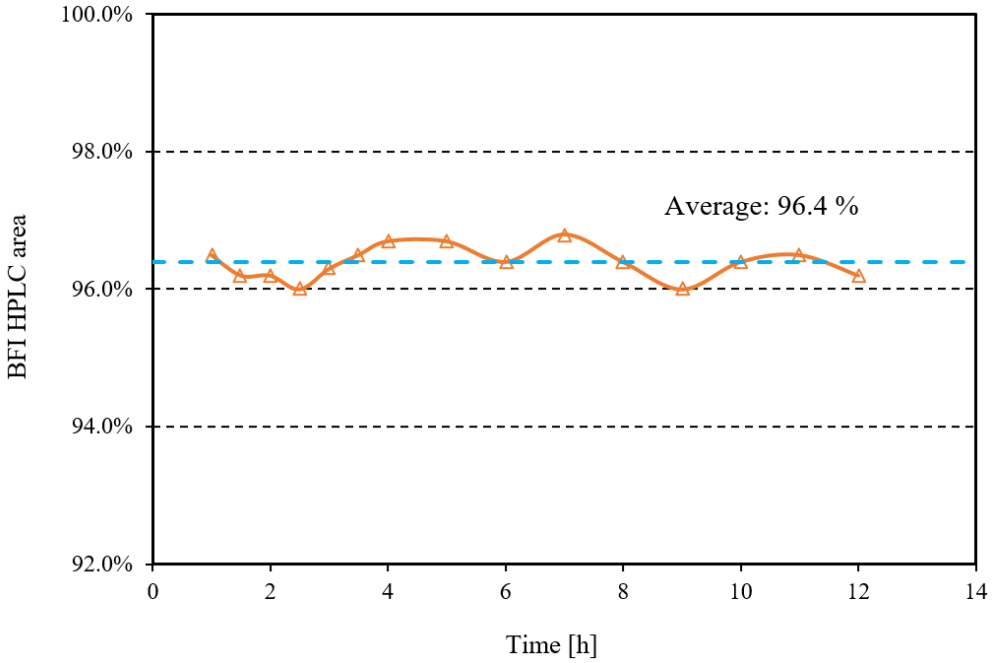

Figure 5. Long-time operation stability test under optimized conditions

Table 5. Observed and predicted reaction results under optimized conditions

Process parameters			HPLC area (%)		Period 1	Period 2
T [°C]	*RT* [min]	*V-ratio*	BFI Observed (Average)	BFI Predicted	BFI Yield	BFI Yield
205	11.1	12.1	96.4%	96.3%	85.6%	85.0%

SUBSTRATE SCOPE

In an attempt to determine the generality of this practical approach, the continuous reactions of several different substituted *o*-fluorobenzaldehydes with *tert*-butyl carbazate (Entries 2-7, Table 6) were evaluated using the conditions found optimal for the synthesis of 6-bromo-4-fluoro-1*H*-indazole (Entry 1,

Table 6). Most of the selected substrates could be operated stably without obvious blockage under continuous-flow mode except the substrate of 4-chloro-2-fluorobenzaldehyde. However, compared with the substrates of 4-bromo-2,6-difluorobenzaldehyde and 2,4,6-trifluorobenzaldehyde, the other substrates could not be converted into the title product of 1*H*-indazoles in good yield. In the case of the synthesis of 4-chloro-1*H*-indazole, only 17.0% yield of title product could be achieved. The intramolecular cyclization of aryl hydrazone to form the anticipated 1*H*-indazole product is considered to be a typical aromatic nucleophilic substitution reaction, in which the electron-withdrawing groups can activate benzene rings for nucleophilic aromatic substitution.[29] The synthesis of 1*H*-indazoles through *o*-fluorobenzaldehydes with *tert*-butyl carbazate is a complex competitive reaction system between the intramolecular cyclization of aryl hydrazone with the side reactions (intermolecular cross condensation of aryl hydrazone with SM or target product, hydroxylation of the reaction component to form phenolic compounds, etc.). The high temperature in the continuous-flow conditions can significantly aggravate these side reactions, resulting the low yield of target products. More electron-withdrawing groups at the aromatic ring (Entries 1 and 2, Table 6) can facilitate the intramolecular cyclization of aryl hydrazone to dominate the competitive reaction system, which may be the key factors for the achievement of satisfactory 1*H*-indazole yields. It is expected that the other substrates can be synthesized in better yields through the decrease of reaction temperature and increase of residence time. Thus, the reaction conditions found optimal for the synthesis of 6-bromo-4-fluoro-1*H*-indazole cannot be directly applied to the other substrates, and further optimizations toward different substrates in a reset range of process conditions were necessary to improve the continuous synthesis process of 1*H*-indazoles.

Table 6. Substrate screening for the continuous synthesis of 1*H*-indazoles

Entry	Substrate	Product	Operability [a]	Yield [%][b]
1	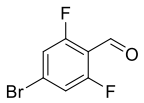	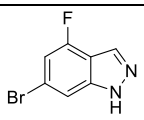	√	85.6
2	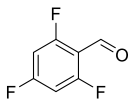	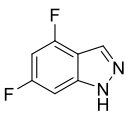	√	76.9
3	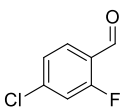	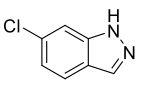	X	N/A
4	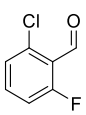	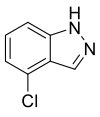	√	17.0

5	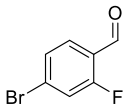	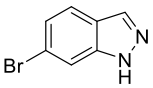	√	18.5
6	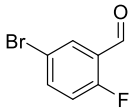	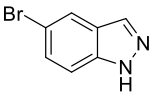	√	7.9
7	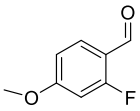	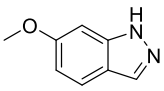	√	4.6

[a] Operability refers to that the system could be operated without obvious blockage. [b] The yields were determined by external standard curve method based on the standard sample.

CONCLUSION

A novel continuous-flow strategy was exploited for the reaction of 4-bromo-2,6-difluorobenzaldehyde with *tert*-butyl carbazate to synthesize 6-bromo-4-fluoro-1*H*-indazole in a highly controlled, safe and efficient manner. Various conditions (reaction temperature, residence time, solvent amount, the amount of *tert*-butyl carbazate, water content) were investigated to elucidate the synthesis of 6-bromo-4-fluoro-1*H*-indazole under continuous-flow conditions. The Box-Behnken design in response surface methodology was employed for the optimization of reaction conditions, and over 85% yield of 6-bromo-4-fluoro-1*H*-indazole could be achieved under optimized condition. A long-time operation stability test (>12 h) under optimized condition was carried out to verify the process reliability. Furthermore, the generality of the reaction conditions found optimal for the synthesis of 6-bromo-4-fluoro-1*H*-indazole was evaluated for the synthesis of several different 1*H*-indazoles.

EXPERIMENTAL

CHEMICALS. 4-Bromo-2,6-difluorobenzaldehyde, 2-fluoro-4-methoxybenzaldehyde, 2-chloro-6-fluorobenzaldehyde, 2,4,6-trifluorobenzaldehyde, 4,6-difluoro-1*H*-indazole, 6-bromo-1*H*-indazole, 4-chloro-1*H*-indazole, 5-bromo-1*H*-indazole, 5-bromo-2-fluorobenzaldehyde, 6-chloro-1*H*-indazole were purchased from Shanghai Bide Pharmatech Ltd. *tert*-Butyl carbazate was purchased from Shanghai D&B Biological Science and Technology Co., LTD. 6-Bromo-4-fluoro-1*H*-indazole, 4-chloro-2-fluorobenzaldehyde, 4-bromo-2-fluorobenzaldehyde, 4-chloro-2-fluorobenzaldehyde, 4-bromo-2-fluorobenzaldehyde, 6-methoxy-1*H*-indazole were purchased from Beijing MREDA Technology Inc. Isopropyl alcohol (*i*-PrOH) and trifluoroacetic acid (TFA) were purchased from Rhawn Chemical Reagent Co., Ltd. Ethanol (EtOH), glycol, tetrahydrofuran (THF), N, N-dimethylformamide (DMF), dimethyl sulfoxide (DMSO), acetonitrile and acetone were purchased

from Shanghai Hushi Chemical Reagent Co., Ltd. N-Methyl-2-pyrrolidone (NMP) was purchased from Shanghai Aladdin Bio-Chem Technology Co., LTD. Methanol (MeOH) was purchased from SEPSERV Berlin Analytik GmbH. Deionized water was prepared in our laboratory and used throughout. All of the chemicals were used without any further purification.

PROCEDURES. A schematic overview of the continuous-flow synthetic system of BFI was shown in Figure 6.

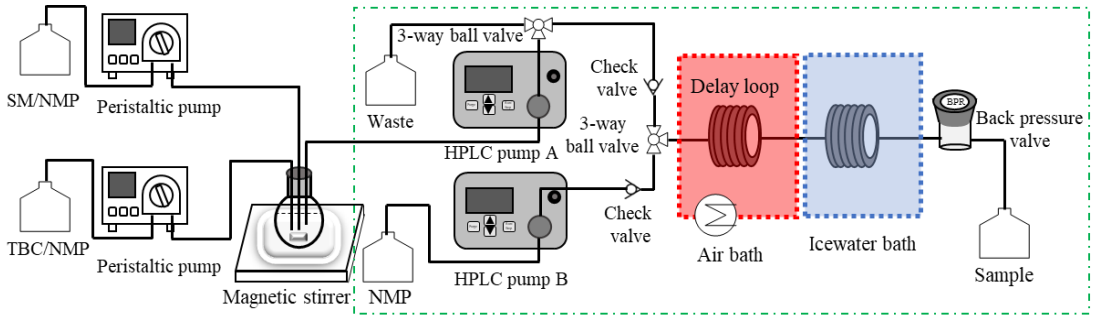

Figure 6. Schematic overview of the continuous-flow synthetic system of BFI

Both SM solution (4-bromo-2,6-difluorobenzaldehyde dissolved in NMP) and *tert*-butyl carbazate solution (*tert*-butyl carbazate dissolved in NMP) were delivered into the system by peristaltic pumps (BT100-1F, Longer Precision Pump Co., Ltd, China.). The two solutions were mixed effectively through the magnetic stirring in a round bottom flask at room temperature to form a mixture of raw material. The residence time in the flask was maintained over 1 h at room temperature and then an equilibrium between SM with aromatic Boc-protected hydrazone could be established. Then the mixture was delivered into the delay loop with an internal diameter of 0.6 mm constructed by stainless steel through the HPLC pump A (Series III pump, Chrom Tech, Inc., Apple Valley, MN, USA). Check valves were installed in the reaction system to prevent the reverse flow of the reactants. The whole delay loop was divided into two sections including reaction section and inhibition section. In the reaction section, the delay loop was immersed in the air bath to control the reaction temperature accurately. In the inhibition section, the delay loop was immersed in the ice water bath to inhibit the reaction. A back-pressure valve with a fixed pressure of 750 psi was installed at the end of the delay loop to ensure the organic solvent was maintained in liquid phase, and simultaneously eliminate the influence of generated gas phase CO_2 on the residence time. The residence time inside the reaction section could be accurately controlled by altering the flow velocity. In the experiments, the samples for analysis were collected after waiting for at least three times the mean residence time associated with the set flow rate, allowing the system to be verified to have reached a steady state. Switching the 3-way ball valve and deliver the solvent NMP into the system by HPLC pump B can check the tightness of the system or clean the reaction system when switch the process

condition or the reactor channel is blocked. Initially, the SM solution and *tert*-butyl carbazate solution delivered by two HPLC pumps were mixed through a T-shaped tee and then flowed into the delay loop. However, obvious blockage phenomenon occurred under high temperature which might due to reason that the reaction is extremely sensitive to the mixing and inefficient mixing will lead to the significant formation of insoluble byproducts. Then the blockage problem could be effectively solved by premixing in a round bottom flask (Figure 6). During the investigation of reaction behavior in our laboratory, the continuous-flow synthetic system was simplified (rectangular box of green dotted line, Figure 1) to simply the experimental procedure and save reaction material. In the experiments, SM and *tert*-butyl carbazate were together dissolved in the solvent of NMP directly, and then the mixture was vigorously stirred to ensure effective mixing and let it stand still for more than 1 h to prepare the starting reaction mixture. It should be noted that the simplification was not recommended during large-scale preparation process due to the presence of the exothermic reaction from SM to aromatic Boc-protected hydrazone.

ANALYSIS. The collected samples were subjected to HPLC analysis to determine the ratio of reaction raw materials, intermediates, targeted products and byproducts. The yields of targeted products were determined by the external standard method (HPLC). Analytical HPLC (EClassical 3100) analysis was carried out on a C18 reversed-phase column (Agilent EC-C18, 150 mm×4.6mm, particle size 5 μm) at 25 ^{o}C using mobile phase A (H_2O+0.05% TFA) and B (MeOH) with a flow rate of 0.8 mL/min (detection at 220 nm). The following gradient was applied: 0 min: A=70%, B=30%; 14 min: A=30%, B=70%; 24 min: A=70%, B=30%; 30 min: A=70%, B=30%.

ACKNOWLEDGEMENTS

We gratefully acknowledge the financial supports for this project from the General Project of Natural Science Research in Colleges and Universities of Jiangsu Province (No. 21KJB530009), the China State Construction Engineering Corp. (CSCEC-2021-Z-51) and Opening Fund of National & Local Joint Engineering Research Center for Deep Utilization Technology of Rock-salt Resource (Grant No. SF202007).

REFERENCES

1. H. Cerecetto, A. Gerpe, M. Gonzalez, V. J. Aran, and C. O. de Ocariz, *Mini-Rev. Med. Chem.*, 2005, **5**, 869.
2. K. Edman, R. Ahlgren, M. Bengtsson, H. Bladh, S. Bäckström, J. Dahmén, K. Henriksson, P. Hillertz, V. Hulikal, A. Jerre, L. Kinchin, C. Kåse, M. Lepistö, I. Mile, S. Nilsson, A. Smailagic, J. Taylor, A. Tjörnebo, L. Wissler, and T. Hansson, *Bioorg. Med. Chem. Lett.*, 2014, **24**, 2571.

3. C. F. Chang, W. H. Lin, Y. Y. Ke, Y. S. Lin, W. C. Wang, C. H. Chen, P. C. Kuo, J. T. A. Hsu, B. J. Uang, and H. P. Hsieh, *Eur. J. Med. Chem.*, 2016, **124**, 186.
4. S. H. Kim, B. Markovitz, R. Trovato, B. R. Murphy, H. Austin, A. J. Willardsen, V. Baichwal, S. Morham, and A. Bajji, *Bioorg. Med. Chem. Lett.*, 2013, **23**, 2888.
5. G. Bellussi, M. Bohnet, J. Bus, K. Drauz, H. Greim, K.-P. Jackel, U. Karst, A. Kleemann, G. Kreysa, T. Laird, W. Meier, E. Ottow, M. Roper, J. Scholtz, K. Sundmacher, R. Ulber, and U. Wietelmann, 'Ullmann's Encyclopedia of Industrial Chemistry, 7th ed.', Wiley-VCH, Weinheim, 2011.
6. K. Lukin, M. C. Hsu, D. Fernando, and M. R. Leanna, *J. Org. Chem.*, 2006, **71**, 8166.
7. P. Schumann, V. Collot, Y. Hommet, W. Gsell, F. Dauphin, J. Sopkova, E. T. MacKenzie, D. Duval, M. Boulouard, and S. Rault, *Bioorg. Med. Chem. Lett.*, 2001, **11**, 1153.
8. S. Tono-oka, Y. Tone, V. E. Marquez, D. A. Cooney, I. Sekikawa, and I. Azuma, *Bull. Chem. Soc. Jpn.*, 1985, **58**, 309.
9. P. Li, J. Zhao, C. Wu, R. C. Larock, and F. Shi, *Org. Lett.*, 2011, **13**, 3340.
10. D. G. Yu, M. Suri, and F. Glorius, *J. Am. Chem. Soc.*, 2013, **135**, 8802.
11. W. McCoull, A. Bailey, P. Barton, A. M. Birch, A. J. Brown, H. S. Butler, S. Boyd, R. J. Butlin, B. Chappell, P. Clarkson, S. Collins, R. M. D. Davies, A. Ertan, C. D. Hammond, J. L. Holmes, C. Lenaghan, A. Midha, P. Morentin-Gutierrez, J. E. Moore, P. Raubo, and G. Robb, *J. Med. Chem.*, 2017, **60**, 3187.
12. J. S. Barber, A. Burtea, M. R. Collins, M. Tran-Dubé, R. L. Patman, S. Scales, G. Smith, J. E. Spangler, F. Wang, S. L. Yang, J. J. Zhu, and T. P. Montgomery, *Org. Lett.*, 2020, **22**, 9047.
13. K. A. Lukin, C. P. Hsu, D. P. Fernando, B. J. Kotecki, and M. R. Leanna, U.S. Patent 20070244178 A1, 2007-10-18.
14. X. R. Wang, S. Wang, W. B. Li, K. Y. Xu, X. P. Qiao, X. L. Jing, Z. X. Wang, C. J. Yang, and S. W. Chen, *Eur. J. Med. Chem.*, 2021, **213**, 113192.
15. T. S. Li, X. D. Zhao, Q. Tian, W. P. Zhang, H. B. Liu, X. L. Wang, H. H. Tan, R. Tan, Q. H. Liu, L. H. Jiang, Y. X. Liu, H. L. Ling, M. Lin, J. Sun, and W. B. Wang, W.O. Patent 2015188777 A1, 2015-12-17.
16. R. Zahler and X. X. Tang, W.O. Patent 2016007837 A1, 2016-01-14.
17. Q. Zeng, M. P. Bourbeau, G. E. Wohlhieter, G. Yao, H. Monenschein, J. T. Rider, M. R. Lee, S. W. Zhang, J. Lofgren, D. Freeman, C. Li, E. Tominey, X. Huang, D. Hoffman, H. Yamane, A. S. Tasker, C. Dominguez, V. N. Viswanadhan, R. Hungate, and X. Zhang, *Bioorg. Med. Chem. Lett.*, 2010, **20**, 1652.
18. M. Baumann, T. S. Moody, M. Smyth, and S. Wharry, *Org. Process Res. Dev.*, 2020, **24**, 1802.
19. A. R. Bogdan and A. W. Dombrowski, *J. Med. Chem.*, 2019, **62**, 6422.

20. L. Rogers and K. F. Jensen, *Green Chem.*, 2019, **21**, 3481.
21. M. B. Plutschack, B. Pieber, K. Gilmore, and P. H. Seeberger, *Chem. Rev.*, 2017, **117**, 11796.
22. J. K. Niemeier and D. P. Kjell, *Org. Process Res. Dev.*, 2013, **17**, 1580.
23. A. R. Bogdan, M. Charaschanya, A. W. Dombrowski, Y. Wang, and S. W. Djuric, *Org. Lett.*, 2016, **18**, 1732.
24. B. T. Brandes and D. K. Smith, *Process Saf. Prog.*, 2016, **35**, 374.
25. G. Li, D. T. Ngo, Y. Yan, Q. Tan, B. Wang, and D. E. Resasco, *ACS Catal.*, 2020, **10**, 12790.
26. G. Wang, C. Li, J. Li, and X. Jia, *Tetrahedron Lett.*, 2009, **50**, 1438.
27. D. C. Montgomery and R. H. Myres, 'Response surface methodology: process and product optimization using designed experiments', John Wiley and Sons, Inc., New York, 2009.
28. S. Sen, U. Mondal, and G. Singh, *Org. Process Res. Dev.*, 2016, **20**, 1765.
29. J. E. McMurry, 'Organic Chemistry, 9th ed.', Cengage Learning, Boston, 2015.